Fatigue Life of Bioactive Titanium Dental Implants Treated by Means of Grit-Blasting and Thermo-Chemical Treatment

F. Javier Gil, PhD;* Eduardo Espinar, DDS, PhD;† Jose Maria Llamas, DDS, PhD;† Pablo Sevilla, PhD*

ABSTRACT

Objective: This study focuses on the fatigue behavior of titanium dental implants as-received, with a grit-blasted surface and with a new bioactive surface treatment (2Steps).

Background: The 2Step process consists of (1) an initial grit-blasting process to produce a micro-rough surface, followed by (2) a combined thermo-chemical treatment that produces a potentially bioactive surface, that is, that can form an apatitic layer when exposed to biomimetic conditions in vitro. The 2Step treatment produced micro-rough and apatitic coating implants.

Methods: Residual stresses were determined by means of X-ray diffraction. The fatigue tests were carried out at 37°C on 500 dental implants, and the S-N curve was determined. The fatigue-crack nucleation for the different treatments was analyzed.

Results: The fatigue tests show that the grit-blasting process improves the fatigue life. This is a consequence of the layer of compressive residual stresses that the treatment generates in titanium surfaces. Dental implants that had its surfaced prepared with the 2Step procedure (grit-blasting and thermo-chemical treatment) had its fatigue life decreased by 10% due to the incorporation of oxygen to the surface and the relaxation of the compressive residual stress produced by the heat treatment.

Conclusions: Thermo-chemical treatment is an excellent compromise between the improvement of bioactive and mechanical long-life behaviors.

KEY WORDS: bioactivity, dental implants, fatigue, titanium

INTRODUCTION

The design of an implantable oral device must always take into consideration the cyclic loads the implant will undergo through its lifetime. The fatigue endurance of the materials used will play a very important role when trying to estimate the long-term performance of the device. Thus, the assessment of the fatigue behavior of implantable alloys has acquired a greater importance.[1–3]

*Bioengineering Research Center (CREB), Department of Materials Science and Metalurgical Engineering, Universitat Politècnica de Catalunya, Barcelona, Spain; †Facultad de Odontología, Universidad de Sevilla, Sevilla, Spain

Reprint requests: Prof. F. Javier Gil, Dept. Ciència dels Materials i Enginyería Metal.lúrgica, ETSEIB, Universitat Politècnica de Cataluña, Avda, Diagonal 647, 08028 Barcelona, Spain; e-mail: francesc.xavier.gil@upc.edu

DOI 10.1111/j.1708-8208.2012.00468.x

The failures of the dental implants are produced, in general, at the two first weeks of the surgery (88%). The causes can be: infection, low osseointegration capacity, increase of bone temperature produced by the drills, poor bone quality, among others. The remaining 12% of the total failures are produced after 6 years of the surgery when the implant has been integrated in the bone for long time. In this case, the failures can be produced by peri-implantitis (10%) or fatigue failures (2%). Consequently, the fatigue life is a very important point to be taken into account when considering the long-term behavior of the dental implants.[4,5]

The surface roughness has been suggested as an important factor in establishing clinically reliable bone attachments.[6–9] Surfaces can be modified by coating, by blasting with various abrasives, by acidic treatment, or by combinations of such treatments. The results from in vitro studies suggest there is a positive correlation between surface roughness and cellular attachment and

osteoblast-like cell activity.[6–8,10] Deposits of osteoconductive calcium phosphate materials such as apatite enhance the implant performance shortly after implantation, because the interface's attachment strength is higher in coated than uncoated implants.[7] There is a dearth of information on the mechanical behavior of coated implants. Particularly critical seems to be the premature detachment of the coatings that may lead to an enhanced release of ions in the biological milieu and to long-term failure of the implant. According to previous works that compared apatite coatings obtained by different methods like plasma spray, laser ablation, the coatings did not last longer than 10^6 cycles in any of the cases. The cause was a rapid propagation of the crack either in the coatings or at the interface with the metal implant.[11–16]

On the other hand, there is an increasing interest in the formation of a bioactive surface layer directly on titanium substrates by chemical treatments in recent years. Such layers have been reported to induce apatite formation in the living environment or simulated body fluid.[1,2] Because the fatigue behavior of a material is closely related to the surface structure, the surface modification methods conducted for osseointegration may affect the fatigue performance of the implant. Furthermore, most chemical surface modification methods require post-thermal processes (heat treatments) that may alter the microstructure of the implant material. This microstructural change might affect the fatigue performance in service. Therefore, these methods must be evaluated with respect to their effects on the fatigue performance of the implant.

The aim of this study is to evaluate the fatigue behavior of as-machined (CTRL), grit-blasted (GB), and a new treatment: rough and bioactive (2Step) commercially pure (c.p.) Titanium (Ti) dental implants.

MATERIALS AND METHODS

Figure 1 shows the macroscopic shape of the implants studied. All implants were machined to the desired dimensions and ultrasonically cleaned during 15 min in acetone and distilled water. Grade 3 titanium dental implants (ASTM B348; Soadco SL, Escaldes Engorgany, Andorra) were used for this study. The dimension of the implants were: length 12 mm, diameters from 3.8 to 4.2 mm and the height of the external hexagon was 1.8 mm. Electropolished implants were treated in a 1:6:9 perchloric-acid:n-butanol:methanol bath at −30°C and 25 V for 4 min.

Figure 1 Illustration of a dental implant used in this study.

Surface Preparations

Three different surface qualities of screw-shaped c.p. Ti dental implants were prepared to determine and compare their behavior in terms of fatigue. They were divided into three groups:

1. as-machined (CTRL);
2. rough-GB (GB), with Al_2O_3 particles of 600 μm in mean size and 0.25 Megapascals (MPa) blasting pressure;
3. rough-GB and bioactive-TCh (2Step), blasted in the same way as GB implants + TCh treatment developed by Kokubo and colleagues.[17] This treatment consists of: (1) introducing the specimen into a vial containing 10 ml of 5 M-NaOH. The vial is placed in an oven at 60°C for 24 h. (2) Careful rinsing with distilled water. (3) Drying at 40°C in an oven for 24 h. (4) Thermal treating in a tubular furnace up to 600°C with a 5°C/min heating-rate for 1 hour. (5) Cooling down inside the furnace to reach room temperature. Each specimen was introduced into a vial containing 40 mL of simulated body fluid[17] (Table 1) and placed in an oven at 37°C for 11 days

TABLE 1 Chemical Composition of the Simulated Body Fluid and Blood Plasma (mM)

	Na^+	K^+	Mg^+	Ca^{2+}	Cl^-	HCO_3^-	HPO_4^-	SO_4^-
SBF	142.0	5.0	1.5	2.5	148.8	4.2	1.0	0.5
Blood plasma	142.0	5.0	1.5	2.5	103.0	27.0	1.0	0.5

SBF = Simulated Body Fluid.

to perform the in vitro testing of their bioactivity. The solution was renewed every 3 days.

Microstructure and Roughness

The implants were examined with an Environmental Scanning Electron Microscopy, Electroscan 2020, including a thermoelectric cooling stage that allowed ± 20°C variations in temperature compared with room temperature. The gas used was water vapor at 5–10 Torr, and the temperature was between 5 and 7°C in order to keep the samples hydratated for as long as possible.

White light interferometry (Wyko NT1100 Optical Interferometer, Veeco Instruments, NY, USA), in its vertical scanning interferometry mode, was used to produce, evaluate, and quantify the topography. The interferometric technique is ideal for imaging these surfaces as a large area of the surface can be imaged with a high vertical resolution (≈2 nm). The analysis area was 124.4 × 94.6 µm. Data analysis was performed with Wyko Vision 32 (Veeco Instruments), which allows the application of a Gaussian filter to separate waviness and form from roughness. Three different specimens of each type were measured to determine the amplitude parameter (S_a), the spacing parameter (S_m), and the hybrid parameter (Index area).

Mechanical Tests

Five standard tensile specimens were tested for each material in a universal screw-driven testing machine (MTS, MN, USA) of 100 kN capacity at a cross-head speed of 1 mm/min in order to obtain the monotic behavior.

The fatigue behavior and the fatigue limit of the prototype were set using the Wöhler's curves (stress – number of cycles) that describe the relation between the amplitude of the cyclical tensions and the number of cycles up to break. During the test, the implant-abutment system was subjected to both cyclical compressive and lateral forces, without any lateral constraint. Five hundred specimens were tested.

The tests were performed in simulated body fluid (17) at 37°C with the servo-hydraulic testing machine MTS Bionix 858, which is specially designed to test biomaterials. This machine was equipped with a load cell MTS of 25 kN and controlled by means of a personal computer equipped with the software TESTAR II® (Silicon Valley, CA, USA).

The tests were performed following the guidelines previously published by the Food and Drug Administration (FDA) at the *Class II Special Controls Guidance Documents: Roots-form Endosseous Dental Implants and Endosseous Dental Implants Abutments* and the ISO 14801:2007. The tested implants supported an abutment that was in line with the axis of the implant. The testing setup clamped the implant so that the implant's long axis made a 30° angle with the loading direction of the testing machine and, consequently, a flexural load was applied (Figure 2). The implants were fixed with a 30-degree inclination from the *z*-axis of the traction-compression machine. A 30-degree angle to the *z*-axis of the tensile-compression machine is recommended by the standards of the FDA as the most unfavorable position. Moreover, the implant was placed 3 mm below the anticipated crestal bone level, simulating 3 mm of bone resorption.

To start with, five resistance tests were conducted, at the selected inclination, to determine the yield strength of the material and the ultimate flexion strength. The different percentages of yield strength that were obtained from these results, ranging from 60 to 90%, were later on used to perform fatigue tests to obtain the number of cycles until fracture.

The aim is to find the level of stress at which the sample supports five million cycles and which will be considered the fatigue limit. Seven of the tests that were carried out to determine the level of stress analyzed the fatigue limit, while three tests analyzed the rest of the tested stresses. The implants were loaded with a sinusoidal function of fatigue at a frequency of 15 Hz, and the relationship between maximum and minimum applied stress was 10%. The tests were performed at room

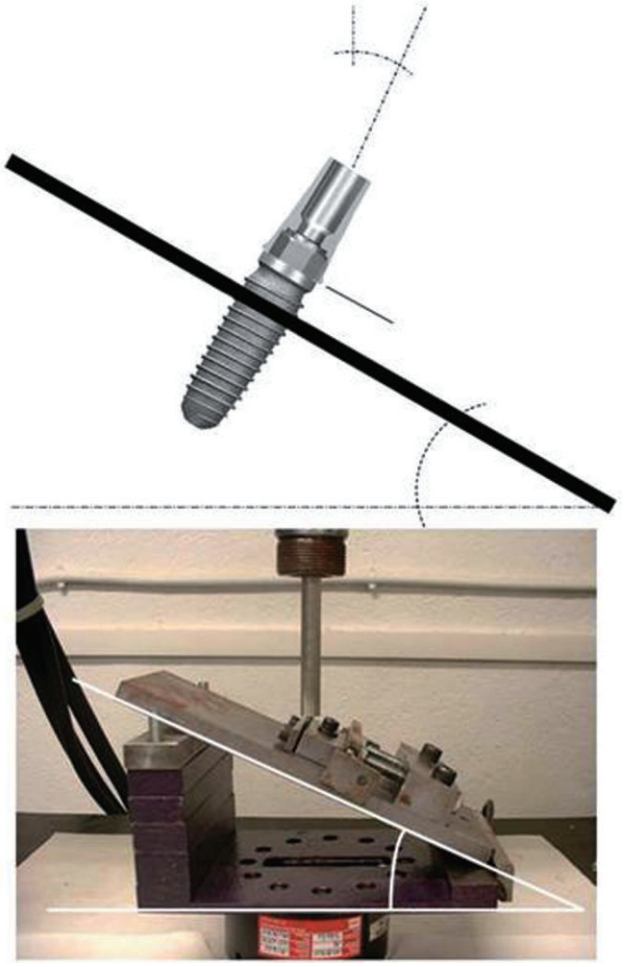

Figure 2 Picture and schematics of the experimental setup and geometrical configuration during fatigue tests.

temperature. The obtained data were represented as number of cycles to failure as a function of applied stress.

Residual Stress

Residual stresses were measured with a difractometer incorporating a Bragg–Bentano configuration (D500, Siemens, Frankfurt, Germany). The measurements were done for the family of planes (213), which diffracts at $2\theta = 139.5°$. The elastic constants of Ti at the direction of this family of planes are Elastic Constants = $(E/1 + \upsilon)_{(213)}$ = 90.3 (1.4) GPa. Eleven ψ angles, 0° and five positive- and five negative-angles were evaluated. The position of the peaks was adjusted with a pseudo-Voigt function using appropriate software (WinplotR, free access online), and then converted to interplanar distances (d_ψ) using Bragg's equation. The $d\psi$ vs. $sen^2\psi$ graphs and the calculation of the slope of the linear regression (A) were done with appropriate software (Origin, Microcal, NJ, USA). The residual stress is: $\sigma = EC * (1/d_0) * A$, where d_0 is the interplanar distance for $\psi = 0°$.

RESULTS

Figure 3 shows the morphology of the different c.p. Ti surfaces with and without thermo-chemical treatment (CTRL, GB, and 2Steps). The GB surfaces show parts of the alumina grit particles adhered to their surface, valleys produced by plastic deformation, and a random roughness without any texture.

Figure 4A illustrates the appearance of a microporous layer made up of an alkaline titanate hydrogel formed during the alkaline/heat treatment described in the materials and methods section above. Figure 4B shows how the first apatite nuclei appeared after 3 days. Figure 4C shows that once the first nuclei had appeared, the growth of the apatite layer was very rapid. In Figure 4D, the surface can be observed completely coated with apatite.

The grazing incidence-X-ray diffraction of a Ti-bioactive surface shows titanium and rutile maxima as well as three more maxima that correspond to two different sodium-titanate stoichiometries, Na_2Ti5O_{11} (JCPDS n°11–0289), and $NaTiO_2$ (JCPDS n°16–0251) (Figure 5). Sodium-titanate and rutile maxima were not observed when the X-ray diffraction patterns were performed under Bragg–Brentano (theta-2 theta) conditions (not shown), which confirms the superficial character of these species.

The apatite layer was obtained after treating the Ti samples with the chemical treatment that was described in the Materials and Methods section. The nature of this deposited layer was characterized by X-ray diffraction (Figure 6). The diffractogram shows a number of peaks at values of around 25° to 34° corresponding to the apatite, while the titanate peaks were gradually disappearing. This result demonstrates the bioactive behavior of the chemical-treated titanium surfaces.[17–19]

The values of the roughness parameters for the different surfaces studied are shown in Table 2. The surface roughness of the CTRL implant was $S_a = 0.21$ (0.02) µm. The GB specimens surface roughness was $S_a = 3.64$ (0.15) µm, and the GB with thermo-chemical treatment was $S_a = 3.55$ (0.45) µm.

The values for the residual stresses are summarized in Table 3. As foreseen, the compressive stresses induced by grit blasting on c.p. Ti are statistically significant

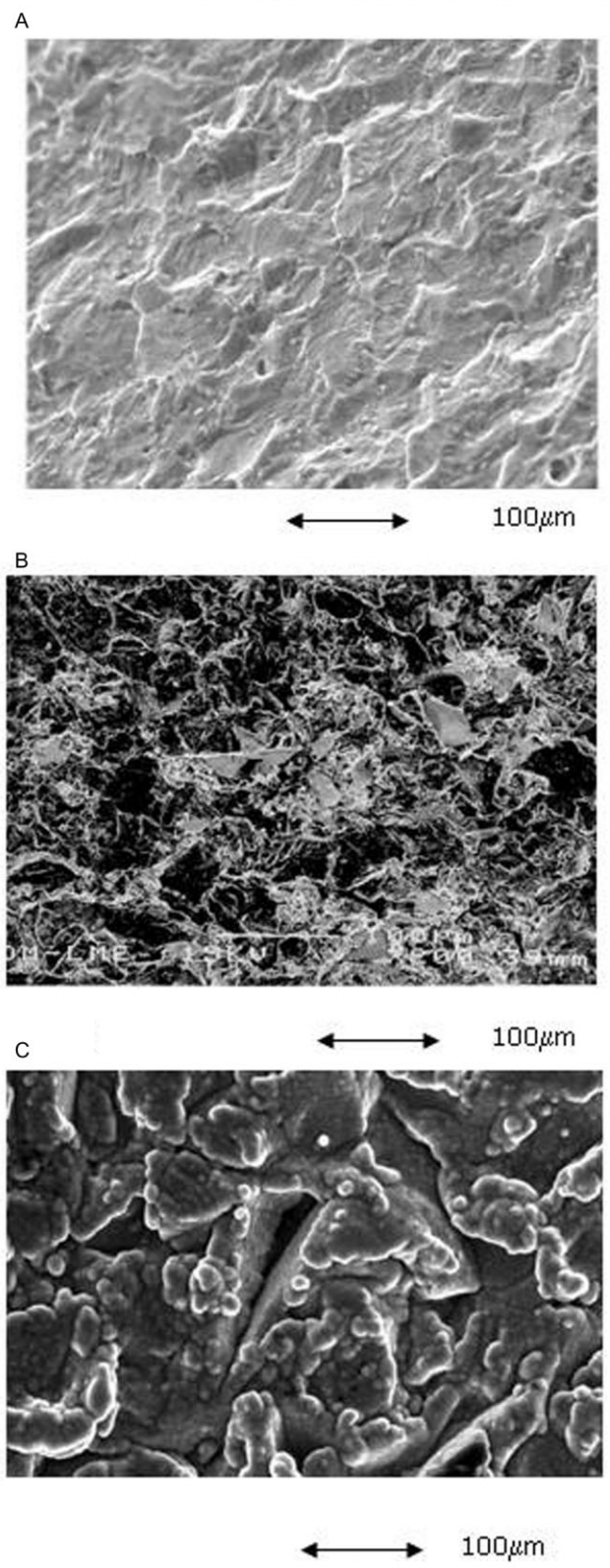

Figure 3 Environmental Scanning Electron Microscopy images of the different treatments applied to the implants. (A) as-received. (B) grit blasting. (C) Grit blasting and thermo-chemical treatment.

TABLE 2 Mean Values ± Standard Deviation of the Roughness Parameters for All Titanium Surfaces Studied. Statistical Differences Are Indicated in the Table ($p < .05$)

Surface	Sa (μm) ± SD	Sm (μm) ± SD	Index Area ± SD
CTRL	0.21 ± 0.02*	0.34 ± 0.02*	1.09 ± 0.01*
GB	3.64 ± 0.15***	5.67 ± 1.07***	2.26 ± 0.05***
2Steps	3.55 ± 0.45***	5.10 ± 1.08***	2.52 ± 0.20***

CTRL = as-machined; GB, grit-blasted; 2Steps = Bioactive; Sa = ampliture parameter; Sm = spacing parameter; SD = standard deviation.
*, **, or *** represent the roughness with statistical differences between them.

($p < .001$, t-Student) and highly different from those induced on CTRL samples, but there are not statistically significant differences between CTRL and GB with thermo-chemical treatment. The residual compressive strength has been eliminated due to the heat treatments needed to obtain the sodium titanate.

The different materials have been tested in unidirectional tension in order to obtain their monotonic stress–strain curves. Cylindrical specimens were used following the international standard for tensile tests. Five samples were tested for each treatment. The relevant parameters are listed in Table 4, with each value being the average of four different tests for each material, as can be observed

TABLE 3 Surface Residual Stresses Calculated at the Four Different Types of c.p. Ti Implants Studied

Material	σ (MPa)
CTRL	−77.2 (5)
GB	−220.0 (3)
2Steps	−12.1 (8)

CTRL = as-machined; GB, grit-blasted; 2Steps = Bioactive; MPa = Megapascals.

TABLE 4 Mechanical Properties Obtained from the Tensile Tests on the Different Materials Studied

Material	Maximum Strength (MPa)	Yield Stress 0.2% (MPa)	Ductility (%)
CTRL	460 (30)	155 (23)	46 (7)
GB	480 (39)	168 (25)	39 (4)
2Steps	517 (34)	179 (23)	17 (3)

CTRL = as-machined; GB, grit-blasted; 2Steps = Bioactive; MPa = Megapascals.

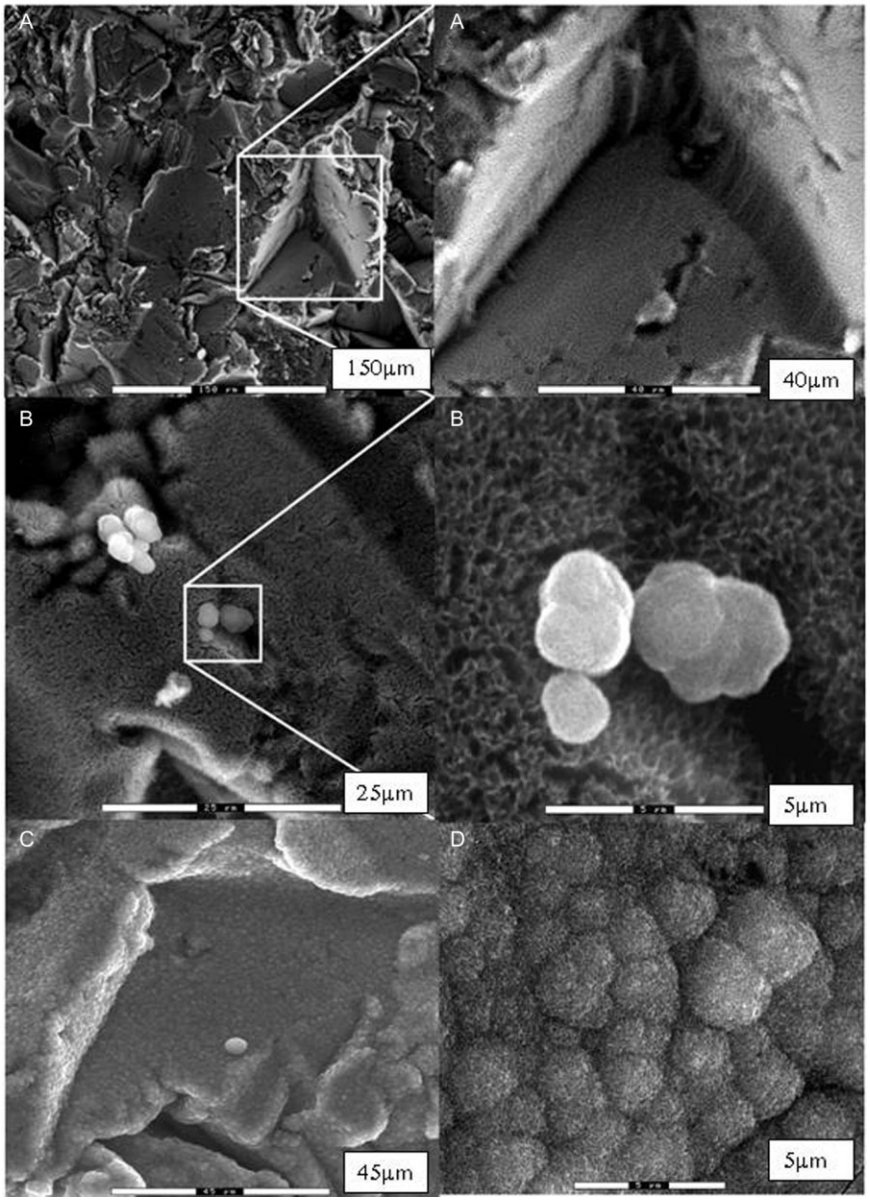

Figure 4 Environmental Scanning Electron Microscopy images showing the (A) original 2S bioactive surface, (B) in vitro nucleation of apatite on 2S surfaces, (C) in vitro formed apatite layer on 2S bioactive surface, and (D) Bioactive surface at more magnification.

the thermo-chemical treatment reduced the ductility of the dental implant. Figure 7 shows the number of cycles before failure (N_f) vs applied load for CTRL, GB, and 2Steps implants. It is evident that the GB presents longer fatigue life than the CTRL and 2Steps samples. The fatigue limit for the GB implants was 350N, CTRL was 330N, and 2Steps was 315N. The samples at this load were tested up to 15 10^6 cycles and they did not show fracture.

DISCUSSION

As expected, the GB specimens with or without thermo-chemical treatment have statistically significant ($p < .001$; t-Student) and higher surface roughness than the CTRL ones. Nonstatistically significant differences in S_a values between the GB specimens were found. The formation of the apatite is homogeneous in the entire surface and did not affect in the roughness. This aspect is important because the roughness obtained (chemical composition and size of grit particles and GB pressure) for the GB c.p. Ti was determined as optimal for in vitro and in vivo response in previous works.[19–22]

A significant result is that GB implants with thermo-chemical treatment significantly reduced the ductility of the alloy; this is due to the oxygen diffusion inside the titanium of the dental implant. The studies by

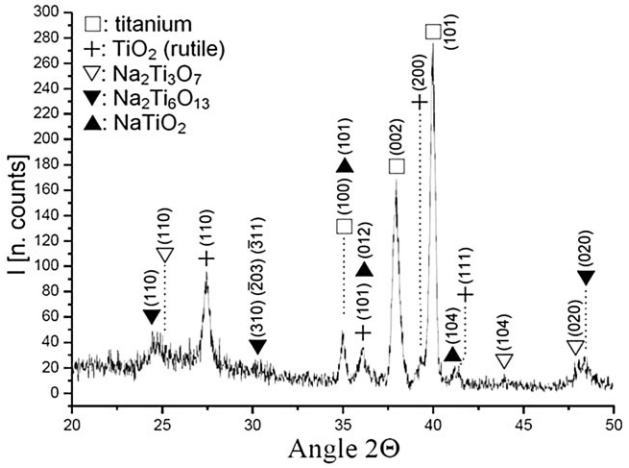

Figure 5 X-ray pattern of the layer deposited on the surface of a Ti-Bio sample, with peaks corresponding to sodium titanates. Joint Committee on Powder Diffraction n. Ti: #44-1294; rutile: #88-1175; $Na_2Ti_3O_7$: #72-0148; $Na_2Ti_6O_{13}$: #73-1398; $NaTiO_2$: #89-2784.

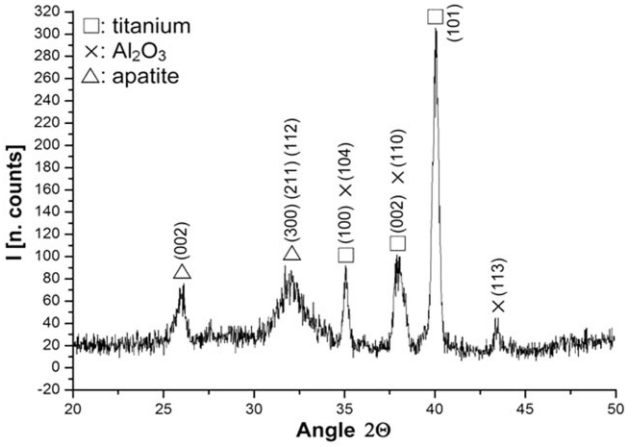

Figure 6 X-ray pattern of the layer deposited on the surface of a AL6-Bio sample, with peaks corresponding to the apatite. JCPDS n. Ti: #44-1294; apatite: #09-0432; Al_2O_3: #89-7717.

means of X Photoelectron Spectroscopy showed that the oxygen content on the 2Steps surfaces increase higher 10 times the as-received implant or GB ones.[19] It is very well known that the introduction of interstitial elements in titanium produces significant increases of the strength and decrease of the ductility.[23,24]

The fatigue behavior of the samples submitted to grit blasting treatment is better due to the compressive effect of the residual stresses on the surface that difficult the crack nucleation. This fact can be observed in Figures 8A (CTRL), 8B (GB), and 8C (2Steps), where the crack grows from the surface for Ctrl and 2Steps specimens and from 10 μm beneath the surface, respectively. As a consequence, an improvement of the fatigue behavior of the GB treatment is achieved.

To sum up, the grit blasting of c.p. Ti dental implants improves not only the osseointegration of the implants due to the increase in the metal surface roughness but also their fatigue life thanks to the layer of compressive residual stresses that is formed. The bioactive implants will produce a reduction in the osseointegration time respect to the grit blasting implants but a reduction in the fatigue life has been demonstrated.

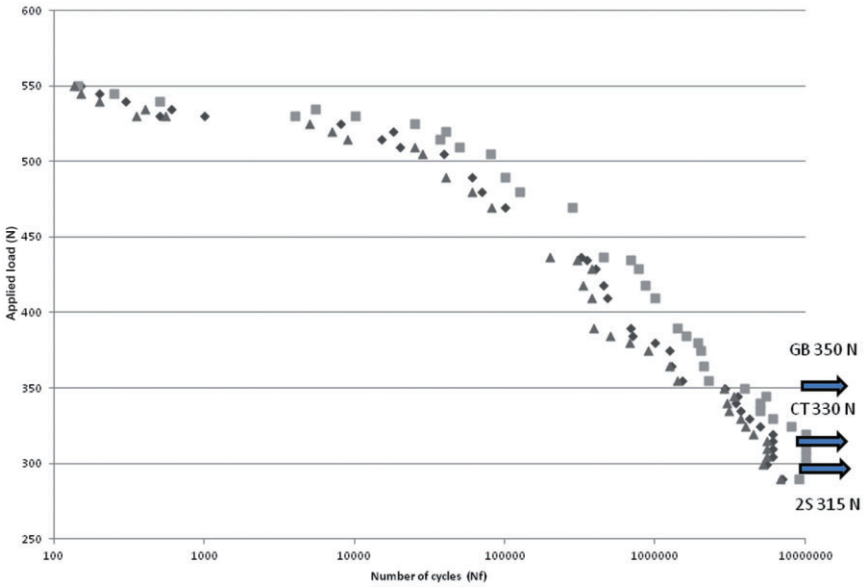

Figure 7 S-N Curve for different types of dental implants. Squares: GB implants, Diamonds: Ctrl implants, Triangles: 2Steps Bioactive implants.

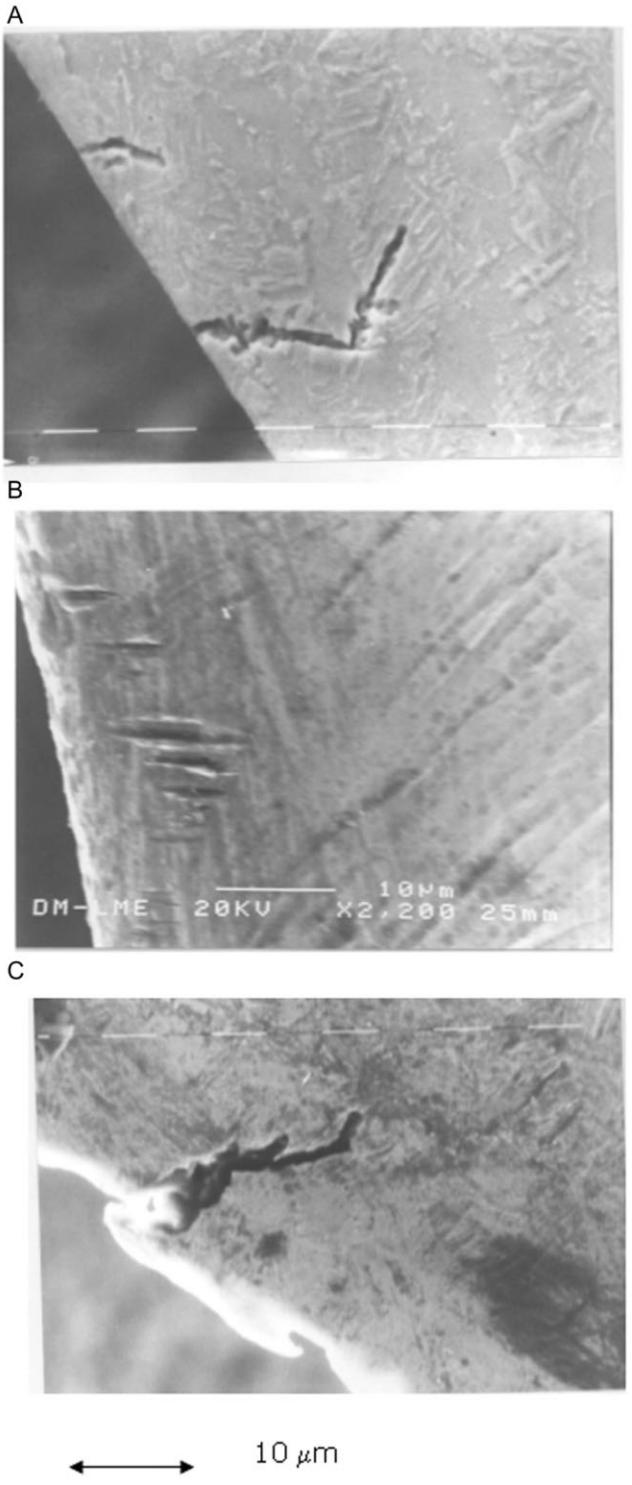

Figure 8 Fatigue crack nucleation: (A) CTRL, (B) beneath the surface of the GB implants, and (C) 2Steps implants.
CTRL = as-machined; GB, grit-blasted; 2Steps = Bioactive.

In comparison with the apatite coatings obtained by plasma spray in air or vacuum or laser deposition, the fatigue life is 10 times higher using thermo-chemical treatment. The poorer performance of long-term apatite coatings has been related to problems in the adhesion of deposits to the substrate and to an improperly controlled dissolution rates of the coatings depending on the level of apatite crystallinity and the higher the potential for degradation.[13–16]

CONCLUSIONS

The thermo-chemical treatment studied reduces fatigue life about 10% in relation to the GB implants. It has been well established that the chemical and postheat treatment affected lightly the fatigue life of the material negatively. The main reason of the decrease in the fatigue performance is the metallurgical stress relieving effect and the incorporation of oxygen in the surface. This treatment kept the microstructure and the roughness. However, the good long life behavior achieved with 2Step treatment is an excellent compromise between osseointegration and fatigue life of the dental implant.

ACKNOWLEDGMENTS

The authors are grateful to the CICYT MAT 13547 and Generalitat de Catalunya (CTP project) for funding the present work and to Klockner, S.L. for kindly donating the material.

REFERENCES

1. Manero JM, Gil FJ, Planell JA. Effect of saline solution environment on the cyclic deformation of Ti-6Al-4V. J Mater Sci Mat Med 1996; 7:131–134.
2. Semlitsch MF, Panic B, Weber H, Schoen R. Comparison of the fatigue strength of femoral prosthesis stems made of forged Ti-Al-V and Cobalt base alloys. In: Luckey HA, Kubli F, eds. Titanium alloys in surgical implants. ASTM-STP796. Philadelphia, PA: ASTM, 1981:120–135.
3. Aparicio C, Gil FJ, Fonseca C, Barbosa M, Planell JA. Corrosion behaviour of commercially pure titanium shot blasted with different materials and sizes of shot particles for dental implant applications. Biomaterials 2003; 24:263–273.
4. Bannon BP, Mild EE. Titanium alloys for biomaterial application: an overview. In: Luckey HA, Kubli F, eds. Titanium alloys in surgical implants. ASTM-STP796. Philadelphia, PA: ASTM, 1981:7–14.
5. Lemons JE. Application of materials in medicine and dentistry. Dental implants. In: Ratner BD, Hoffman AS, Schoen FJ, Lemons JE, eds. Biomaterials Science: an introduction to materials in medicine. San Diego, CA: Academic Press, 1996:308–318.
6. Giavaresi G, Fini M, Cigada A, et al. Mechanical and histomorphometric evaluations of titanium implants with different surface treatments inserted in sheep cortical bone. Biomaterials 2003; 24:1583–1594.

7. Ronold HJ, Lyngstadaas SP, Ellingsen JE. Analysing the optimal value for titanium implant roughness in bone attachment using a tensile test. Biomaterials 2003; 24:4559–4564.
8. Albrektsson T, Branemark PI, Hansson HA, Lindstrom J. Oseeointegrated titanium implants. Requirements for ensuring a long-lasting direct bone-to-implant anchorage in man. Acta Orthop Scand 1981; 52:155–170.
9. Buser D, Schenk RK, Steinemann S, Fiorellini JP, Fox CH. Influence of surface characteristics on bone integration of titanium implants. A histomorphometric study in miniature pigs. J Biomed Mater Res 1991; 25:889–902.
10. Han CH, Johansson CB, Wennerberg A, Albrektsson T. Quantitative and qualitative investigations of surface enlarged titanium and titanium alloys implants. Clin Oral Implant Res 1998; 9:1–10.
11. Chang YL, Lew D, Park JB, Keller JC. Biomechanical and morphometric analysis of hydroxyapatite-coated implants with varying crystallinity. Int J Oral Maxillofac Surg 1999; 57:1096–1108.
12. Cabrini M, Cigada A, Rondelli G, Vicentini B. Effect of different surface finishing and of hydroxyapatite coatings on passive and corrosion current of Ti6Al4V alloy in simulated physiological solution. Biomaterials 1997; 18:783–787.
13. Chang YL, Lew D, Park JB, Keller JC. Biomechanical and morphometric analysis of hydroxyapatite-coated implants with varying crystallinity. J Oral Maxillofac Surg 1999; 57:1096–1108.
14. Shrikhanzadeh M. Bioactive calcium phosphate coating prepared by electrodeposition. J.Mater Sci Lett 1991; 10:1415–1417.
15. Hulshoff JEG, Hayakawa T, van Dijk K, Lejidekkers-Govesr AFM, van der Waerden JPCM, Jansen JA. Mechanical and histologic evaluation of Ca-P plasma spray and magnetron sputter-coated implants in trabecular bone of the goat. J Biomed Mater Res 1997; 36:75–83.
16. Geesink RGT, de Groot K, Klein CPAT. Chemical implant fixation using hydroxyl-apatite coatings. Clin Orthop 1987; 225:147–170.
17. Kokubo T, Miyaji F, Kim HM. Preparation of bioactive Ti and its alloys via simple chemical surface treatment. J Am Ceram Soc 1996; 79:1127–1129.
18. Aparicio C, Engel E, Gil FJ, Planell JA. Human-osteoblast proliferation and differentiation on grit-blasted and bioactive titanium for dental applications. J Mater Sci Mater Med 2002; 13:1105–1111.
19. Aparicio C, Gil FJ, Thams U, Muñoz F, Padrós A, Planell JA. Osseointegration of grit-blasted and bioactive titanium implants: histomorphometry in minipigs. Key Eng Mat 2004; 254–256:737–740.
20. Wennerberg A, Albrektsson T, Johansson C, Andersson B. Experimental study of turned and grit-blasted screw-shaped implants with special emphasis on effects of blasting material and surface topography. Biomaterials 1996; 17:15–22.
21. Buser D. Titanium for dental applications (II): implants with roughened surfaces. In: Brunette DM, Tengvall P, Textor M, Thomsen P, eds. Titanium in medicine: material science, surface science, engineering, biological responses and medical applications. Berlin: Springer Verlag, 2001:875–888.
22. Predecki P, Stephan JE, Auslander BA, Mooney VL, Kirkland K. Kinetics of bone growth into cylindrical channels in aluminium oxide and titanium. J Biomed Mater Res 1972; 6:375–400.
23. Svehla M, Morberg P, Zicat B, Bruce W, Sonnabend D, Walsh WR. Morphometric and mechanical evaluation of titanium implant integration: comparison of five surface structures. J Biomed Mater Res 2000; 51:15–22.
24. Tengvall P, Lundtröm I. Physico-chemical considerations of titanium as a biomaterial. Biomaterials 1992; 9:115–134.